Multi-scale Drivers of Spatial Variation in Old-Growth Forest Carbon Density Disentangled with Lidar and an Individual-Based Landscape Model

Rupert Seidl,[1,2]* Thomas A. Spies,[3] Werner Rammer,[2] E. Ashley Steel,[4] Robert J. Pabst,[1] and Keith Olsen[1]

[1]Department of Forest Ecosystems and Society, College of Forestry, Oregon State University, Corvallis, Oregon, USA; [2]Institute of Silviculture, Department of Forest and Soil Sciences, University of Natural Resources and Life Sciences (BOKU), Vienna, Austria; [3]USDA Forest Service, Pacific Northwest Research Station, Corvallis, Oregon, USA; [4]USDA Forest Service, Pacific Northwest Research Station, Seattle, Washington, USA

ABSTRACT

Forest ecosystems are the most important terrestrial carbon (C) storage globally, and presently mitigate anthropogenic climate change by acting as a large and persistent sink for atmospheric CO_2. Yet, forest C density varies greatly in space, both globally and at stand and landscape levels. Understanding the multi-scale drivers of this variation is a prerequisite for robust and effective climate change mitigation in ecosystem management. Here, we used airborne light detection and ranging (Lidar) and a novel high-resolution simulation model of landscape dynamics (iLand) to identify the drivers of variation in C density for an old-growth forest landscape in Oregon, USA. With total ecosystem C in excess of 1 Gt ha^{-1} these ecosystems are among the most C-rich globally. Our findings revealed considerable spatial variability in stand-level C density across the landscape. Notwithstanding the distinct environmental gradients in our mountainous study area only 55.3% of this variation was explained by environmental drivers, with radiation and soil physical properties having a stronger influence than temperature and precipitation. The remaining variation in C stocks was largely attributable to emerging properties of stand dynamics (that is, stand structure and composition). Not only were density- and size-related indicators positively associated with C stocks but also diversity in composition and structure, documenting a close link between biodiversity and ecosystem functioning. We conclude that the complexity of old-growth forests contributes to their sustained high C levels, a finding that is relevant to managing forests for climate change mitigation.

Key words: forest carbon storage; old-growth forests; climate change mitigation; ecosystem structure and functioning; functional diversity; forest stand dynamics; airborne Lidar; individual-based modeling; iLand.

Authors Contributions: RS designed the study, developed the model, performed the research, analyzed the data, and wrote the paper; TAS contributed to study design, data analysis, and writing; WR contributed new methods and models, assisted in research and data analysis, and contributed to writing; EAS contributed new methods and models, and helped writing the paper; RJP assisted in performing the research and analyzing the data, and contributed to writing the paper; KO assisted in performing the research and analyzing the data.

*Corresponding author; e-mail: rupert.seidl@boku.ac.at

INTRODUCTION

Forest ecosystems store more than 800 Pg carbon (C) globally (Pan and others 2011), which corresponds approximately to the amount of C stored in the earth's atmosphere. The C density (C stored per unit area) of forest ecosystems varies considerably in space, both globally (Pan and others 2011) and at the stand and landscape scale (Bradford and others 2010). The highest C densities are generally found in old-growth forests, that is, ecosystems that have not been subject to stand replacement disturbance for a significant amount of time. Thus, despite their decreasing global extent, old-growth forests are crucially important for gaining insight into the regulation and upper bounds of forest ecosystem C storage.

Multiple drivers acting at different hierarchical levels affect C cycling in forest landscapes. Climatic factors are frequently reported as major drivers of spatial variation (for example, Turner and others 1996; Baccini and others 2004). It can be hypothesized that—especially in complex mountainous terrain—variation in climate in general, and in temperature and precipitation in particular, are primary drivers of spatial variation in C storage. Yet, Stegen and others (2011) found only weak support for an influence of climate on the variability in forest C storage in a recent meta-analysis of climate–carbon relationships. While climate (together with soil processes) sets the stage for the ecological play to unfold, processes at lower hierarchical levels (for example, the interactions among trees as the main actors in forest ecosystems) also contribute to the stand-level variation in C storage.

Stand structure and composition, which are emergent properties (sensu Levin 1998) of stand dynamics (that is, the interplay of tree-level processes such as growth, mortality, regeneration, and competition), are important indicators in this regard. Hardiman and others (2011), for instance, reported the influence of canopy structure on productivity and C sequestration to be equally strong as site effects. Likewise, species composition was found to influence the C cycle (for example, Hooper and Vitousek 1997; Balvanera and others 2005; Yachi and Loreau 2007), with higher evenness in species and forest types generally associated with higher and more stable C uptake (Bradford 2011). However, a detailed characterization of forest structure and composition across landscapes has been historically difficult, and has become available only recently through advances in remote sensing (for example, Kane and others 2011).

Furthermore, studies addressing the effect of structure and composition have largely focused on differences between seral stages of forest succession (Runyon and others 1994; Turner and others 2003), which leads us to hypothesize that within a given seral stage of stand development processes of stand dynamics have little influence on the stand-level variation in C density.

In general, the relative importance of top-down constraints (climate, soil) and bottom-up emerging properties (structure, composition) in explaining the variation of forest C density at the stand level remains poorly understood (Baraloto and others 2011). Yet the C stored in forest ecosystems has a distinct influence on the climate system, which makes understanding its drivers an increasingly important question in the context of mitigating anthropogenic climate change (Canadell and Raupach 2008). Of particular relevance in this context is the role of climatic drivers of C stocks (cf. robustness to future climatic changes), and the potential to improve forest C stores via the management of stand structure and composition. Understanding how these factors influence C densities is thus a prerequisite for developing effective and robust mitigation strategies in ecosystem management (see McKinley and others 2011).

Here, our aims were to (i) characterize the spatial variation in forest ecosystem C density in an old-growth forest landscape, and (ii) identify the main factors influencing stand-scale variation in C storage across the landscape. We selected old-growth forests in the western Cascade Range of Oregon (USA) as our study system because they are characterized by complex terrain (that is, considerable environmental variability at relatively small scales), and are among the most C-dense terrestrial ecosystems globally (Smithwick and others 2002). We used light detection and ranging (Lidar) in combination with ground survey data to describe the spatial variation in landscape-level C stores. To address the hierarchical nature of influences in forest ecosystems and disentangle effects of both climatic constraints and emergent stand properties, we used a novel multi-scale landscape model with individual tree resolution.

MATERIALS AND METHODS

Material

HJ Andrews Experimental Forest

The HJ Andrews Experimental Forest (HJA) is located at N44.2°, W122.2° in the western Cascade

Range of Oregon. It encompasses the entire 6364 ha drainage basin of Lookout Creek. The watershed is characterized by steep mountainous topography and well-drained soils derived from aeolian volcanic materials, colluvium, and residual materials from Tertiary basalts and andesites. The maritime climate has wet, mild winters and dry, cool summers. Mean monthly temperatures at lower elevations range from near 1°C in January to 18°C in July. Precipitation falls primarily from November to March, and varies with elevation, averaging 2300 mm at low elevations to over 3550 mm at higher elevations per year.

Lower elevation forests are dominated by Douglas-fir (*Pseudotsuga menziesii* (Mirb.) Franco), western hemlock (*Tsuga heterophylla* (Raf.) Sarg.), and western redcedar (*Thuja plicata* Donn ex D. Don). Upper elevation forests contain noble fir (*Abies procera* Rehd.), Pacific silver fir (*Abies amabilis* Dougl. ex Forbes), Douglas-fir, and western hemlock, with a mid-elevation transition zone situated between these two forest types. Low- and mid-elevation forests in this area are among the tallest and most productive in the world, with average canopy heights in excess of 75 m. Under natural conditions, Douglas-fir is a seral dominant on these sites and typically develops young, nearly pure, even-aged stands after severe fires. Stands over 200 years old generally exhibit old-growth characteristics (Spies and Franklin 1988) such as codominance of western hemlock in the overstorey, diverse vertical foliage distribution, and large accumulations of coarse woody debris (Spies and others 1988).

When it was established in 1948, the Andrews Experimental Forest was about 65% old-growth forest (much of that was ~500 years old) with the remainder largely in mature stands (80–200 years old) that developed after wildfires in the mid-1800s to early 1900s. About 30% of the original forest cover has been clear cut, creating plantations of native conifers. Historically, high to mixed severity wildfire was the primary disturbance in the natural forest with return intervals of 80 to over 200 years.

Soil and Climate Data

Soil data for the HJA were available from 326 soil profiles (Dyrness 2001), and were imputed to the soil mapping units (that is, soil series × slope class) of Dyrness and others (2005). After rastering to a 100 m grid missing data were derived by means of ordinary kriging (Figure 1). In addition to C and nitrogen (N) pools for mineral soil and forest floor, soil physical properties (sand, silt, and clay content as well as effective rooting depth, that is, the minimum of soil depth sans rock fraction and potential maximum rooting depth, with the latter set to 250 cm) were derived from soil profile data. A proxy of nutrient availability (plant-available N per hectare and year) was calculated from total N pools following the approach of Seidl and others (2012). Except for the C and N pools, which were dynamically simulated in our study (see below), all soil properties were assumed to be time-invariant.

A daily climate time series from 1973 to 2001 was available for the PRIMET weather station located in the southwestern part of the landscape (Daly and McKee 2009). Furthermore, using an extended network of meteorological stations throughout the HJA watershed, spatial grids of monthly temperature (Daly and Smith 2005a), precipitation (Daly 2005), and radiation (Daly and Smith 2005b) have been developed previously. These data were used to determine regions of homogeneous climate by means of cluster analysis. Using scree-plots of within-cluster dissimilarity, cluster silhouette, and cluster isolation (Kaufman and Rousseeuw 1990; R Development Core Team 2011), we determined that the optimal number of climate regions was 113. We used monthly differences and ratios to the PRIMET climate to generate daily climate data for the representative grid cell (that is, cluster medoid, the representative data point with minimal within-cluster dissimilarities) for every region (Figure 1).

A 500-year time series was created for every climate region by stratified sampling with replacement from the observation period 1973–2001, using the Pacific Decadal Oscillation (PDO) index as stratification criterion. We classified years in the observation period into cool, neutral, and warm PDO phases (see also Tepley 2010), and sampled years from the respective subset following the PDO reconstruction of MacDonald and Case (2005) for the period 1501–1972. A time series of atmospheric CO_2 concentration change from 1765 to 2001 was obtained from Meinshausen and others (2011), and a constant atmospheric CO_2 concentration of 280 ppm was assumed prior to 1765.

Vegetation Data

Two wall-to-wall layers of vegetation data were used in the analysis: first, spatially explicit information on vegetation structure and composition were derived from gradient nearest neighbor (GNN) imputation of forest inventory data (Ohmann and others 2011). Specifically, stand basal area (BA), quadratic mean diameter (QMD),
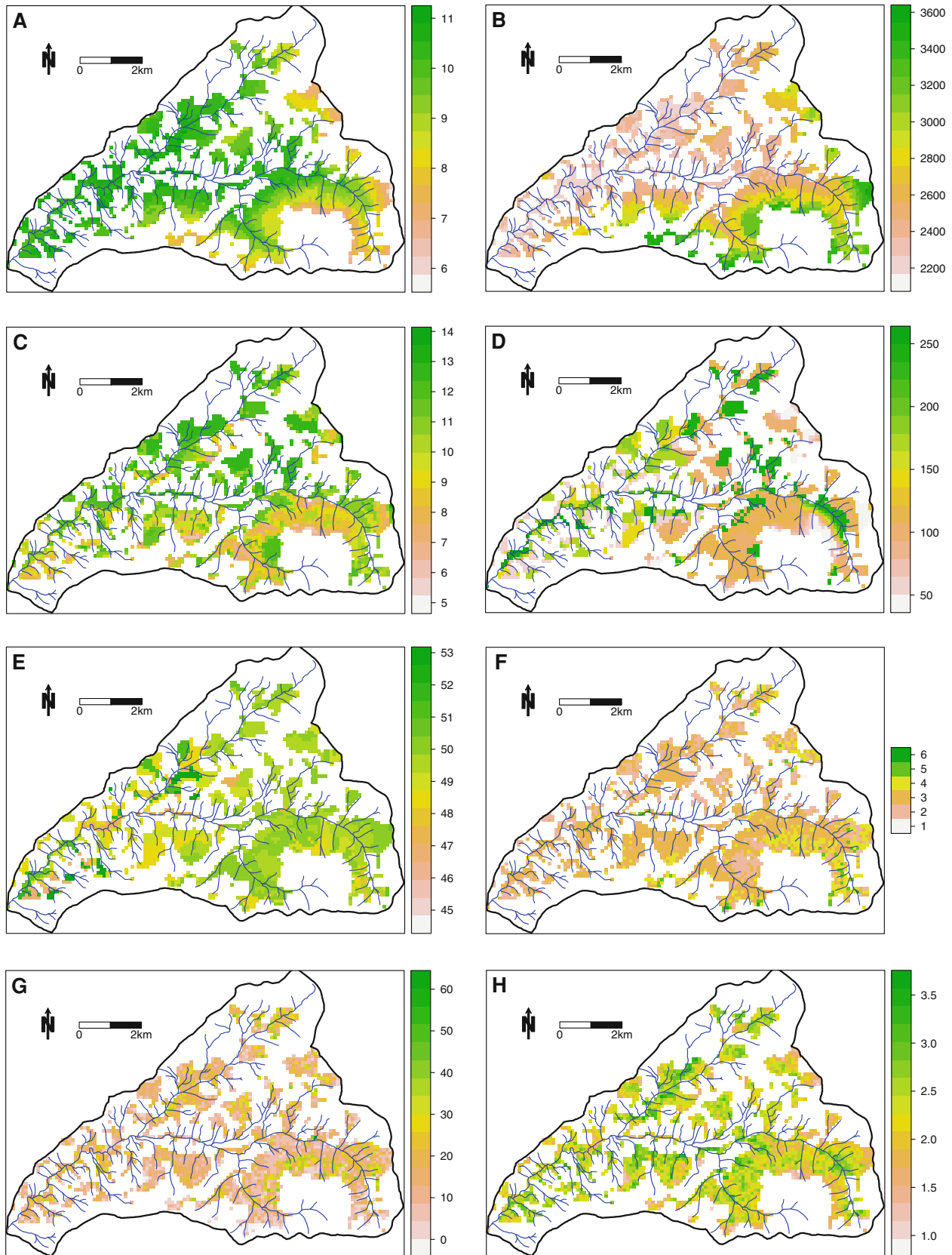
◄ **Figure 1.** Spatial variation of environmental drivers (**A–E**) and stand structure and composition (**F–G**) in the old-growth forests of the HJ Andrews Experimental Forest. **A** Mean annual temperature (°C), **B** mean annual precipitation (mm y^{-1}), **C** mean daily radiation (MJ m^{-2} d^{-1}), **D** effective rooting depth (cm), **E** plant-available nitrogen (kg ha^{-1} y^{-1}), **F** dominant species richness (n ha^{-1}), **G** trees larger than 100 cm dbh (n ha^{-1}), **H** rumple index (dimensionless). Climate data are averages for the period 1973–2001, soil data are assumed to be time-invariant. All maps are masked to old-growth forests within the HJ Andrews watershed (*bold black line*). For more details on stand structure and composition see Table 1. (Color figure online)

the standard deviation of the diameter distribution (SD$_{dbh}$), the abundance of trees larger than 100 cm diameter at breast height (N$_{100}$), and tree species proportion, richness, and diversity were derived from GNN data (Table 1).

Second, airborne discrete return Lidar data (see Lefsky and others 2002) were collected on August 10 and 11, 2007 by Watershed Sciences, Inc. (Corvallis, Oregon, USA). Lidar was collected by a fixed wing aircraft equipped with a Leica ALS50 Phase II laser scanner with a 59 kHz pulse rate, scan angle of ±14°, and scan swath overlap of at least 50%. Average Lidar point return density exceeded 9 m^{-2} within the study area, and root

mean squared error between 344 real-time kinematic ground survey points and Lidar data was 0.024 m. The 95th percentile height (H_{95}) of Lidar returns was created using the "Gridmetrics" command in FUSION (McGaughey 2011). Statistics were processed from the original Lidar point cloud (first returns only) and summarized to 5 m raster cells. From H_{95}, we calculated an index of canopy structure, that is, the rumple index (Parker and others 2004; Kane and others 2010), using the surfaceArea command in R (Bivand and others 2008). Rumple is the ratio of the canopy surface-Area to the projected surface ground area, and was calculated for each 100 m grid cell (Table 1). We used Lidar data in combination with detailed on-site vegetation data to derive estimates of above-ground C density (see "Methods" section).

Delineation of Old-Growth Forests

Our analysis here focused on the old-growth portion of the HJA watershed. To identify old-growth forests, we compiled a fire history for the landscape, building on detailed disturbance history studies by Teensma (1987), Weisberg and Swanson (2003), and Tepley (2010). In addition, we used orthophoto imagery from the 1950s and current Lidar data to corroborate and amend the last 100 years of these previous tree-ring-based fire

Table 1. Spatial Variation in Forest Structure and Composition at the HJ Andrews Experimental Forest

	5th percentile	Mean ± SD	95th percentile
Structure[1]			
Basal area (BA, m^2 ha^{-1})	37.5	59.9 ± 12.6	76.9
Quadratic mean dbh (QMD, cm)	21.8	35.2 ± 8.7	49.4
SD of dbh distribution (SD$_{dbh}$, cm)	14.3	24.3 ± 5.9	33.7
Trees >100 cm dbh (N$_{100}$, n ha^{-1})	2.8	14.8 ± 8.5	30.4
Rumple index (rumple, dim.)	1.61	2.32 ± 0.40	2.96
Composition[1,2]			
Psme (% basal area)	37.5	62.4 ± 15.6	88.2
Tshe (% basal area)	6.3	22.0 ± 10.8	42.4
Thpl (% basal area)	0.0	10.0 ± 9.3	28.2
Abam (% basal area)	0.0	3.0 ± 5.6	14.8
Abpr (% basal area)	0.0	1.3 ± 3.5	7.6
Acma (% basal area)	0.0	0.6 ± 1.6	3.2
Alru (% basal area)	0.0	0.4 ± 2.0	1.4
Tsme (% basal area)	0.0	0.3 ± 1.1	1.9
Dom. species richness (SP$_{rich}$, n ha^{-1})	2.0	2.9 ± 0.8	4.0
Species diversity[3] (SP$_{div}$, dim.)	0.32	0.50 ± 0.14	0.79

SD = standard deviation; dbh = diameter at breast height; Psme = Pseudotsuga menziesii; Tshe = Tsuga heterophylla; Thpl = Thuja plicata; Abam = Abies amabilis; Abpr = Abies procera; Acma = Acer macrophyllum; Alru = Alnus rubra; Tsme = Tsuga mertensiana.
[1]*Data are reported for 2191 ha of old-growth forests and analyzed at the level of 100 m grid cells.*
[2]*The analysis is restricted to species with a share of ≥5% on total basal area in at least one vegetation plot of the survey by Harmon and Munger (2005), and additionally excludes Castanopsis chrysophylla for parameterization reasons. The species proportions, richness of dominant species (>5% of basal area), and species diversity reported here are calculated for the thus selected eight main canopy species.*
[3]*Simpson's diversity index (McGarigal and others 2002).*

history reconstructions. Spatial information on forest management was available from Lienkaemper ([2004](#)). We focused our analysis on the portion of the landscape that was neither managed nor affected by moderate or high severity wildfires since approximately 1800. Via this definition of old-growth, we selected 2191 ha (that is, approximately one-third of the overall HJA watershed) as our study area.

Methods

Estimating Aboveground C Density from Lidar Data

Field data were assembled from a variety of previous vegetation-related projects at HJA (see Harmon and Munger [2005](#)), and consequently were of different plot sizes and clustered over the landscape. From field data on tree size and abundance per 25 m by 25 m plot aboveground live C (ALC) was derived by means of allometric equations. To increase the robustness of this ALC estimate, we used the average over two different sets of allometric equations (Means and others [1994](#); Jenkins and others [2004](#)). Because biomass estimates represent volumes and are skewed, they were cube-root transformed. Because the 708 plots were clustered in space, they were divided into 41 reasonably spatially independent groups before analysis. Potential predictors included aspect, elevation, and metrics created from the Lidar data representing tree height and its horizontal as well as vertical variability (that is, the mean, variance, and 95th percentile of Lidar return heights, the percentage of returns >2 m and 40 m above ground, two indices based on canopy cover, as well as the spatial variance of the 95th percentile Lidar return height in 15, 25, 35, and 45 m cells around the focal 5 m pixel). To identify the best set of predictor variables, simple linear regression models were built using the average of the cube-root transformed data for each of the 41 groups as the response. The best model was selected using a modified forward selection procedure. To correctly account for the hierarchical structure of the plot data, final model coefficients and standard errors were estimated using 100,000 iterations of a non-parametric bootstrap in which groups were re-sampled with replacement (Davison and Hinkley [1997](#)).

iLand: The Individual-Based Forest Landscape and Disturbance Model

To test hypotheses about interacting drivers (that is, environment, stand dynamics) of spatial variation in C density, we used the simulation model iLand

(Seidl and others [2012](#)). iLand models forest ecosystems from a complex adaptive systems perspective (see Grimm and others [2005](#)), with ecosystem dynamics an emergent property of interactions between agents (that is, individual trees) and their environment. The spatially explicit competition for resources between individuals is simulated based on ecological field theory (see Berger and others [2008](#)). The computational challenge of simulating (a large number of) individual trees at the landscape scale is addressed by defining competitive influence as generalized interference patterns in the model (Seidl and others [2012](#)). To robustly scale from individual trees to forest landscapes iLand employs a hierarchical multi-scale approach (Wu and David [2002](#), Figure [2](#)). Within this framework, generalized physiological principles are applied to calculate individual tree growth and mortality from the resources captured by every individual. iLand employs a light-use efficiency approach to model primary production (Landsberg and Waring [1997](#)), and scalar modifiers to account for effects of temperature, soil water availability, and humidity (on daily basis), as well as the effects of nutrient availability and atmospheric CO_2 concentration (on monthly basis). Allocation to tree compartments is based on empirical allometric ratios (Duursma and others [2007](#)), and height to diameter growth relations are determined by an individuals' competitive situation (Seidl and others [2010](#)). The probability of stress-related mortality is calculated from an individuals' C balance (Güneralp and Gertner [2007](#)).

iLand was previously successful in simulating productivity and complex stand dynamics over wide environmental gradients for a number of different species and ecosystems, including the HJA (Seidl and others [2012](#)). To adapt the model to the needs of this study, and develop it into a full dynamic landscape simulator, we integrated a soil module and a regeneration module into the iLand simulation framework. The soil and decomposition module, described in detail in Appendix A of the Supplementary material, tracks dead organic matter in separate pools for standing and downed deadwood, litter, and soil organic matter (Kätterer and Andren [2001](#)). The sensitivity of decomposition processes to climate is modeled based on the empirical findings of Adair and others ([2008](#)). The regeneration module (details in Appendix B of Supplementary material) simulates spatially explicit seed dispersal in the landscape, using a two-part exponential dispersal kernel (Lischke and Löffler [2006](#)). Species-specific thermal limitations to establishment are modeled based on a phenology
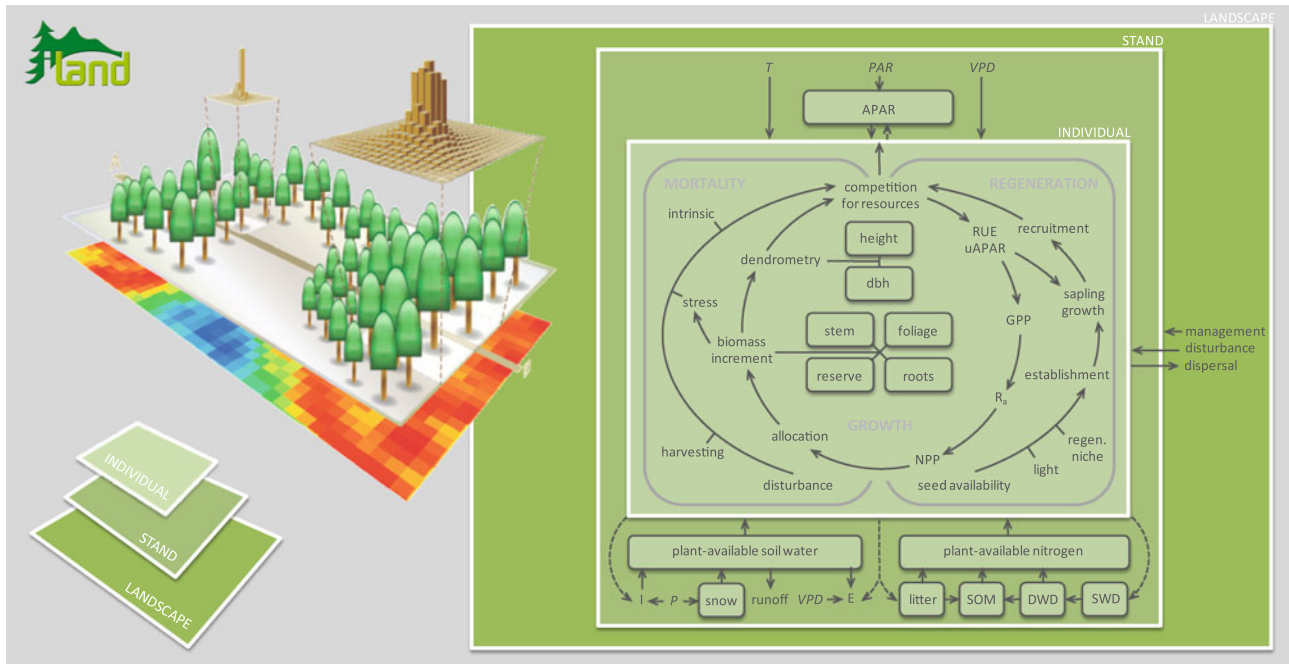
Figure 2. iLand, the individual-based forest landscape and disturbance model. The schematic (*left*) illustrates iLands' approach to scale competition via dynamically combining species- and size-specific individual tree light interference patterns (*top*) to a continuous landscape scale field of light competition (*bottom*). The flowchart to the *right* highlights the main processes and their respective scales (*square boxes*) in the hierarchical multi-scale design of iLand. *Rounded boxes* denote state variables or pools, external environmental drivers are given in *italics*, and *arrows* indicate causal influences or relationships between processes, with *dashed* connections highlighting main feedbacks between hierarchical scales. T mean temperature; T_{min} minimum temperature; *PAR* photosynthetically active radiation; *VPD* vapor pressure deficit; *P* precipitation; *APAR* absorbed PAR; *uAPAR* utilizable APAR; *LUE* light use efficiency; *GPP* gross primary production; R_a autotrophic respiration; *NPP* net primary production; *I* interception; *E* transpiration; *SOM* soil organic matter; *DWD* downed woody debris; *SWD* standing woody debris. (Color figure online)

approach (Nitschke and Innes 2008), while the detailed light computations in iLand (Seidl and others 2012) account for the light regime experienced by seedlings. Sapling growth and competition are modeled explicitly at a 2 × 2 m resolution using a mean tree approach based on height growth potentials (Rammig and others 2006) and species-specific responses to the environment. Extensive technical model documentation as well as the model code and executable are available online at http://iland.boku.ac.at.

Study Design and Analysis

We used Lidar estimates to quantify ALC stocks and their variation at stand level (that is, a 100 m grid), and employed simulations to extend our analysis to total ecosystem C (TEC, up to a maximum soil depth of 100 cm, not including C in lichens and the herb layer). Spatial variation in C density was analyzed by means of both non-spatial [coefficient of variation (CV), 5th to 95th percentile range (R_{90})] and spatially explicit (patch density, division index, see

Jaeger 2000; McGarigal and others 2002) indices. To account for the hierarchy of influences in forest ecosystems in disentangling the drivers of spatial C variation, we performed two hierarchically nested analysis steps: first, we conducted a full factorial simulation experiment, in which we—separately and in combination—fixed temperature, precipitation, radiation, soil physical properties, and N availability to their respective landscape averages. The resulting 32 model runs were analyzed by means of an analysis of variance to quantify the relative contribution of these environmental drivers to the variation in C density (R_{90}) at the stand scale (100 m resolution in our analysis). Second, we analyzed the residual variation not accounted for by environmental drivers for effects of stand dynamics and its emergent properties stand structure and composition. Explanatory variables in this second analysis step were the indicators listed in Table 1. Principal component regression analysis was used to address the correlation in predictors in relating indices of structure and composition to C density.

Table 2. Parameter Estimates for the Lidar—Aboveground Live Carbon Model

Parameter[1]	Estimate[2]	Lower 90% CI[2]	Upper 90% CI[2]
Intercept	0.187	0.0880	0.277
H_{95}^{3} (m)	0.0211	0.0191	0.231
Elevation (m)	0.000198	0.000117	0.000278
LV_{7}^{4} (m²)	0.000177	−0.0000202	0.000365

CI = confidence interval.
[1]*The model assumes a linear combination of parameters with the cube root of aboveground live biomass (Mg) at 25 m² cells as response variable. Aboveground live carbon was derived by assuming a C content of 50%.*
[2]*Derived from 100,000 iterations of a nonparametric boostrap in which groups of spatially dependent observations were resampled with replacement.*
[3]*95th percentile Lidar return height.*
[4]*Variance in H_{95} across a 35 m × 35 m area centered on the focal 5 m cell.*

iLand simulations were started in the year 1501, that is, immediately following the last known landscape level high severity fire event (Tepley 2010). Location and extent of patches surviving the disturbance were taken from the analysis of Tepley (2010). In those legacy patches (∼10% of the study area) vegetation was initialized using stand information for current old-growth stands (Harmon and Munger 2005). On the remaining, burnt-over part of the landscape these data were combined with consumption rates from the literature (for example, Campbell and others 2007) to initialize dead wood pools. Current soil and litter pools were assumed (Dyrness 2001) and were likewise modified with consumption rates for the portion of the landscape initialized as recent burn. Simulations were run for 500 years and the full 6364 ha HJA landscape. The results presented here focus on the old-growth portion of the simulated landscape (2191 ha) at the end of the 500-year simulation period. Because parts of the simulation model used here were newly developed we also conducted a suite of model evaluation experiments prior to applying iLand to our study questions (Appendix C of the Supplementary material). All statistical and spatial analyses were conducted using the R Project for Statistical Computing (R Development Core Team 2011).

RESULTS

Aboveground Live C

The best regression model to predict ALC from Lidar, determined using the simple linear models, included three predictors: H_{95}, elevation, and the local variance of Lidar returns within a 35 m × 35 m window (that is, the approximate dimensions of the ground survey plots) centered on the focal 5 m pixel (LV_7). Although the bootstrapped confidence interval might not support the continued inclusion of LV_7 in the final model, we have retained it because it was significant in the simple linear model based on group means. Model coefficients for H_{95} and elevation are nearly identical when LV_7 is included and when LV_7 is not included in the final model. The average adjusted R^2 for the final regression model (Table 2) across all 100,000 bootstrapped samples was 0.768.

Our Lidar-based ALC estimates corroborated very high C stocks for old-growth forests at the HJA (see for example, Smithwick and others 2002), with a mean ALC density of 435.1 Mg ha^{-1} and a 95th percentile ALC of 667.3 Mg ha^{-1}. The highest ALC stocks (≥95th percentile) were predominantly found on gentle slopes (between 20 and 40% inclination) with southerly or westerly exposition in the mid-elevation range (between 900 and 1100 m asl) of the landscape (Figure 3). Lidar data also revealed considerable spatial variation in old-growth forest C density: the CV in stand-level ALC was 34.3%, and both patch density and division index were high, signifying variability at small spatial scales (Table 3).

Total Ecosystem C

iLand was able to reproduce observed indicators of forest structure and composition at HJA, and simulated ALC levels closely matched Lidar-based values (see Table 3 and the detailed analyses in Appendix C of the Supplementary material). Mean TEC densities for old-growth forests were calculated to be on average 66% higher than ALC densities, with a 95th percentile landscape TEC of 999.4 Mg ha^{-1}. On average, litter and soil contributed 20.6%, woody detritus 15.5%, and live roots 9.8% to TEC. The spatial variation in TEC (CV = 26.2%) was lower than for ALC, but spatially explicit diversity indices were high also for total C (Table 3; Figure 3).
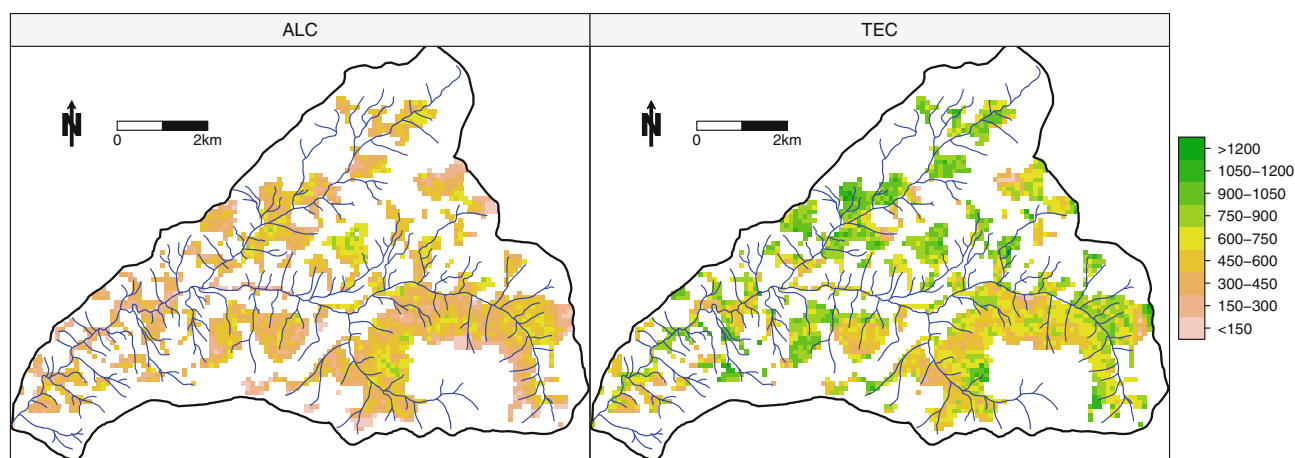
Figure 3. Aboveground live carbon (ALC, derived from Lidar) and total ecosystem carbon (TEC, simulated with iLand) in old-growth forests at the HJ Andrews Experimental Forest (Mg C ha^{-1}). (Color figure online)

Table 3. Carbon Storage in Old-Growth Forests of the HJ Andrews Experimental Forest

		ALC (Lidar)	ALC (iLand)	TEC (iLand)
Central tendency	Mean (Mg C ha^{-1})	435.1	396.5	724.5
Variation (Spatially non-explicit)	R_{90}[1] (Mg C ha^{-1})	496.7	428.2	583.5
	CV[2] (%)	34.3	34.9	26.2
Variation (Spatially explicit)[3]	Patch density[4] (100 ha^{-1})	22.1	18.1	26.5
	Division index[5] (dim.)	0.995	0.981	0.995

ALC = aboveground live carbon; TEC = total ecosystem carbon.
[1]*90th percentile range (that is, the range between the 5th and 95th percentile of landscape C density).*
[2]*Coefficient of variation.*
[3]*Results were grouped into 150 Mg C ha^{-1} classes to identify homogeneous patches (see Figure 3).*
[4]*Number of patches per 100 ha (McGarigal and others 2002).*
[5]*The probability that two randomly chosen places in the landscape are not situated in the same undissected patch (Jaeger 2000); the minimum division index from separate calculations for all C classes is reported here.*

Drivers of Spatial Variation in C Density

Lidar-based ALC densities were only weakly correlated with individual environmental drivers, with radiation and effective soil rooting depth being the most prominent factors (Figure 4). A stronger relationship was found with individual indicators of stand structure, with Lidar-based ALC moderately correlated to vertical and horizontal heterogeneity (that is, rumple index and SD$_{dbh}$) as well as size and stocking level (N$_{100}$ and BA). However, because of the hierarchical nature of influence (coincident effect of environment on both stand dynamics and ecosystem productivity) and the multicollinearity between individual factors these correlations allow only limited insight into the processes driving variation in C density of old-growth forests at HJA.

We thus conducted a full factorial simulation experiment with a process-based model to disentangle environmental effects from the influence of stand dynamics on C density. We found that variation in environmental drivers was responsible for 55.3% of the spatial variation in TEC density (53.8% for ALC). Radiation was identified as the most important environmental driver (Figure 5A). According to our analysis, solar energy thus had a stronger influence on C storage than climatic factors limiting plant metabolism (for example, temperature) in the mountainous terrain of HJA. Furthermore, soil physical properties (that is, the local ability to store water) were found more influential on variation in C than the overall amount of precipitation. Precipitation is generally high throughout the landscape (see Figure 1B) but is unevenly distributed over the year, with a distinct dry season in summer, which makes the ability to store precipitation and runoff from snow-melt a crucial parameter for plant growth in (solar energy-rich) early summer.

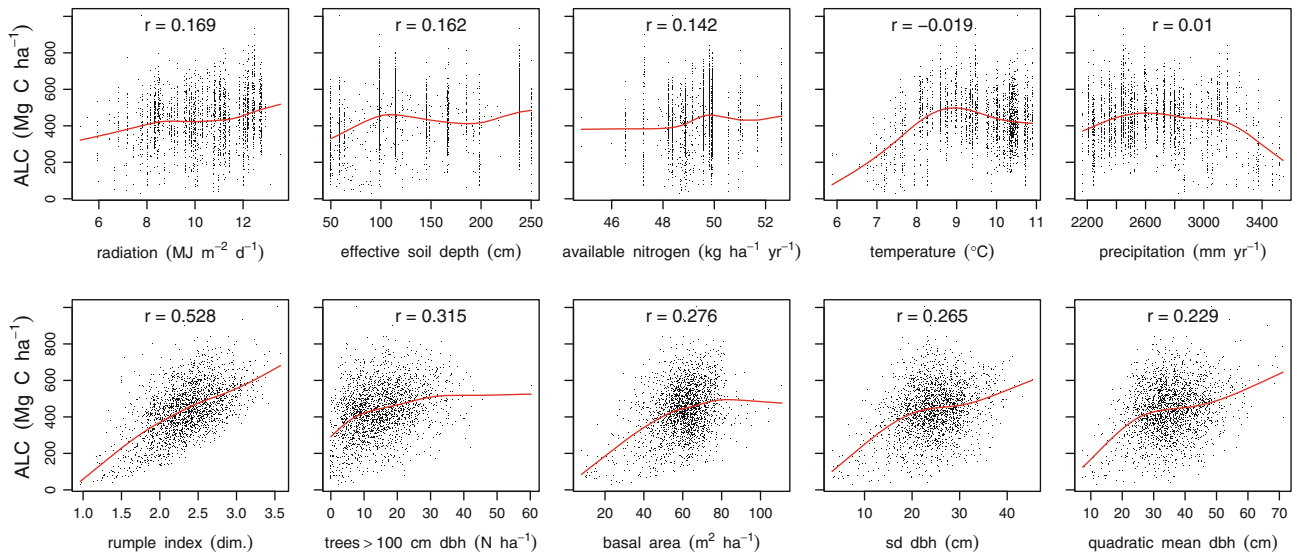In a subsequent step, we analyzed how much of the C variation not explained by environmental

Figure 4. Correlations between Lidar-derived aboveground live C (ALC) density and environmental drivers (*top row*) as well as indicators of stand structure and composition (*bottom row*). For the latter, the five strongest relationships from the list of indicators described in Table 1 are reported. Note that rumple index was derived from the same data source used to estimate ALC. *Red lines* are spline fits drawn to aid interpretation, r Pearson's correlation coefficient. (Color figure online)
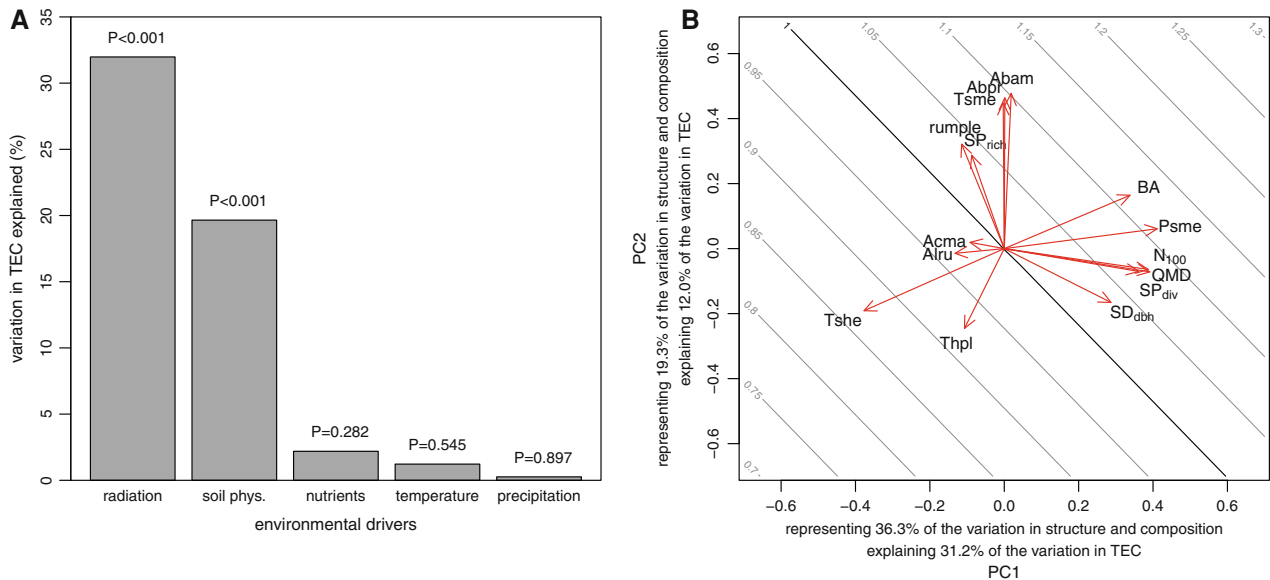

Figure 5. A Environmental drivers of spatial variation in total ecosystem carbon (TEC) density, derived from an analysis of variance based on a full factorial simulation experiment with iLand. **B** Principal component analysis of the influence of structure and composition on TEC. Isolines were derived from coefficients of a principal component regression and indicate the change in TEC relative to its mean value with the change in the first two principal components (PC). *Arrow* length denotes factor loadings. *Soil phys.* soil physical properties; see Table 1 for description and abbreviations of structure and composition indicators.

drivers was attributable to stand structure and composition. Using simulations sans environmental variation allowed us to control not only for direct but also indirect effects of environmental drivers (via influence on stand dynamics) on C density in

our analysis. Together, indicators of stand structure and composition explained at least two thirds of the remaining spatial variation in C density (R^2 of the principal component regression of 0.665 (TEC) and 0.931 (ALC), respectively). As expected, density-

and size-related indicators of stand structure (for example, BA, number of big trees) showed a strong positive relationship with C density (Figure 5B). But also species richness was positively associated with C density, in particular, in relation to an increasing share of true fir species in mid- and high-elevation stands. An increasing share of shade-tolerant *T. heterophylla* and *T. plicata*, on the other hand, associated with climax stages of stand development and a senescing of the dominant *P. menziesii* cohort, were negatively related to C stocks. Principal component analysis showed that compositional diversity is closely related to structural diversity in our study landscape. Our analysis indicates that diversity in canopy and diameter structure had a moderate positive relation to C density.

DISCUSSION

Spatial C Variation and Its Drivers

We analyzed the spatial variation in C density in a mountain forest landscape in western Oregon, and found that stand-level C stocks vary substantially even in the absence of stand-replacement disturbance. In contrast to studies relating C budgets primarily to temperature and precipitation (for example, Govind and others 2011), we found that the effect of solar energy input (strongly mediated by topographic features like slope, aspect, and elevation in our study landscape) and the buffering capacity of soil with regard to water availability were major environmental drivers of C density variations at HJA. These results suggest that total C storage in these old-growth landscapes might be at least initially resistant to future changes in temperature and precipitation. But further analyses accounting for the effect of large-scale disturbances (and their climate sensitivity) need to be conducted to corroborate this notion.

We, furthermore, found that the explanatory power of stand structure and composition (emergent properties of stand dynamics) was in the same order of magnitude as that of the abiotic environment, that is, top-down and bottom-up processes together drive stand-level variation in C densities. Not only density- and size-related indicators of stand structure but also the structural and compositional diversity of stands was positively associated with C density in our analyses, documenting a positive relationship between biodiversity and ecosystem functioning. Our data suggest that one mechanism behind this finding is complementary resource use (species with different traits and

strategies optimize resource use, Hooper and Vitousek 1997; Yachi and Loreau 2007), particularly in the species-rich mid- to high-elevation true fir zone. Furthermore, the (temporal and spatial) scale of analysis matters; although peak C densities might be found in small, relatively homogeneous patches with a high density of large *P. menziesii*, a trade-off with increasing vulnerability of such conditions to disturbance exists at broader scales (see, for example, Seidl and others 2011). Our finding that the long-term integral of C storage is positively associated with diversity indicators suggests a stabilizing effect of diversity, if considering century-scale forest dynamics at the landscape level. This finding is congruent with the theoretical consideration that the response diversity introduced by heterogeneity (Elmqvist and others 2003) is an important constituency of ecosystem resilience. We conclude that typical old-growth features such as complex canopy structure, a considerable number of big trees, and high species diversity are not only important for habitat quality (see for example, Spies and others 2007) but also relevant in the context of ecosystem C storage. In this regard, our findings support the notion that objectives of conserving biodiversity and mitigating climate change through C storage could be mutually achieved in some situations (see Huston and Marland 2003; Seidl and others 2007).

Methodological Limitations and Implications

An aspect not considered in our analysis but potentially contributing to spatial variation in C density is long-term legacies of disturbance of various kinds and intensities. Disturbance can have a long-lasting influence on ecosystem structure and composition, for example, through favoring the regeneration of long-lived early seral species such as *P. menziesii*, or creating slowly decaying pulses of woody debris (see Franklin and others 2002). Despite our focus on forests unaffected by major disturbances in the past 200 years, effects of older disturbances cannot be completely ruled out. Furthermore, it is also likely that some of the structural variation we see is a result of lower severity fire disturbances, small-scale windthrow, and Douglas-fir bark beetles (*Dendroctonus pseudotsugae*). Because such local and low severity disturbances as well as fine scale environmental factors (for example, local rock outcrops, seepages, and small streams) were not accounted for explicitly in our study, forest structure and composition as considered here can only be seen as a surrogate for stand dynamics.

Further limitations of our analysis stem from the applied modeling methodologies. The relationship between ALC determined from ground plot data and Lidar returns was satisfactorily strong and in the range of previous Lidar-derived C models (for example, Lefsky and others 2005). However, the data used to build the empirical model were collected for other purposes. Empirical biomass estimates collected using a sampling scheme designed specifically for building C models could improve the ability to predict biomass and C in unsampled locations in the future. iLand, although employing general physiological process understanding and operating at higher spatial- and process-resolution than most current landscape simulation models, simplifies important C cycle processes such as autotrophic and heterotrophic respiration, compared to more detailed models (see Appendix A of the Supplementary material for details). The high influence of radiation in our results might be somewhat inflated by the structure of the model, which relies on radiation as the principal driver of primary production (light-use efficiency approach). However, the independent Lidar-based analysis of ALC resulted in findings congruent with simulations (Figure 4), adding support to the result that radiation is the most important environmental driver of heterogeneity at HJA. A further limitation of the model is that the lateral components of the water cycle (for example, subsurface water flow) are currently not simulated explicitly (but see Tague and others 2009). However, a thorough model evaluation in general and the good agreement between the two independent ALC estimates (empirical Lidar modeling, simulation modeling) in particular lend confidence to the applied methods and their abilities in the context of our study objectives (see Appendix C of the Supplementary material).

An important methodological implication of the study arises from its reinforcement of the links between structure and functioning in forest ecosystems (Franklin and others 2002; Balvanera and others 2005). The effects of structure and composition on C density documented here highlight the importance of considering the emergent properties of stand dynamics explicitly in making model predictions about the forest C cycle. This finding is in line with the analysis by Smithwick and others (2003), who found that complex nonlinear interactions of small-scale processes (such as for example, competition) and their associated emerging behaviors matter for the prediction of ecosystem dynamics at larger scales (see also Grimm and others 2005)

CONCLUSIONS

We characterized the spatial variation in C density for a C-rich forest ecosystem and investigated what drives this variation. We found that environmental factors were indeed the overall most important drivers of C variation. However, in contrast to large-scale studies (for example, Runyon and others 1994) our findings at landscape scale suggest that radiation and soil characteristics, both strongly mediated by the complex topography of our study landscape, contribute more to the variance in C density than air temperature and precipitation. Furthermore, making use of emerging remote sensing products and novel high-resolution modeling allowed us to extend our analysis to include the effects of stand dynamics (that is, of local processes such as individual-tree competition, mortality, and establishment) on large-scale C density, and to address the interaction between ecosystem structure and functioning. Despite focusing on forests in the same seral stage (old-growth forests), we found that effects of stand dynamics were in the same order of magnitude as those induced by the strong environmental gradients of the mountainous landscape studied. Our results suggest that typical old-growth features, for example, an abundance of large individuals as well as structural and compositional diversity, are positively associated with C density. Our findings on a positive relationship between diversity and C density could be important in the context of the emerging interest to manage forests in the context of climate change mitigation (McKinley and others 2011) and underline the significance of complexity for forest ecosystem functioning.

ACKNOWLEDGMENTS

REFERENCES

Adair EC, Parton WJ, Del Grosso SJ, Silver WL, Harmon ME, Hall SA, Buke IC, Hart SC. 2008. Simple three-pool model accurately describes patterns of long-term litter decomposition in diverse climates. Glob Change Biol 14:2636–60.

Baccini A, Friedl MA, Woodcock CE, Warbington R. 2004. Forest biomass estimation over regional scales using multisource data. Geophys Res Lett 31:L10501.

Balvanera P, Kremen C, Martinez-Ramos M. 2005. Applying community structure analysis to ecosystem function: examples from pollination and carbon storage. Ecol Appl 15:360–75.

Baraloto C, Rabaud S, Molto Q, Blanc L, Fortunel C, Herault B, Davila N, Mesones I, Rios M, Valderrama E, Fine PVA. 2011. Disentangling stand and environmental correlates of above-ground biomass in Amazonian forests. Glob Change Biol 17:2677–88.

Berger U, Piou C, Schiffers K, Grimm V. 2008. Competition among plants: concepts, individual-based modeling approaches, and a proposal for a future research strategy. Perspect Plant Ecol Evol Syst 9:121–35.

Bivand RS, Pebesma EJ, Gómez-Rubio V. 2008. Applied spatial data analysis with R. New York: Springer. 374 pp.

Bradford JB. 2011. Divergence in forest-type response to climate and weather: evidence for regional links between forest-type evenness and net primary productivity. Ecosystems 14:975–86.

Bradford JB, Weishampel P, Smith ML, Kolka R, Birdsey RA, Ollinger SV, Ryan MG. 2010. Carbon pools and fluxes in small temperate forest landscapes: variability and implications for sampling design. For Ecol Manage 259:1245–54.

Campbell J, Donato D, Azuma D, Law B. 2007. Pyrogenic carbon emission from a large wildfire in Oregon, United States. J Geophys Res 112:G04014.

Canadell JG, Raupach MR. 2008. Managing forests for climate change mitigation. Science 320:1456–7.

Daly C. 2005. Average monthly and annual precipitation spatial grids (1980–1989), Andrews Experimental Forest. Long-term ecological research. Forest Science Data Bank, Corvallis, OR. http://www.andrewsforest.oregonstate.edu/data/abstract.cfm?dbcode=MS027. Accessed October 05, 2011.

Daly C, McKee W. 2009. Meteorological data from benchmark stations at the Andrews Experimental Forest. Long-term ecological research. Forest Science Data Bank, Corvallis, OR. http://www.andrewsforest.oregonstate.edu/data/abstract.cfm?dbcode=MS001. Accessed October 05, 2011.

Daly C, Smith J. 2005a. Mean monthly maximum and minimum air temperature spatial grids (1971–2000), Andrews Experimental Forest. Long-term ecological research. Forest Science Data Bank, Corvallis, OR. http://www.andrewsforest.oregonstate.edu/data/abstract.cfm?dbcode=MS029. Accessed October 05, 2011.

Daly C, Smith J. 2005b. Radiation spatial grids, Andrews Experimental Forest. Long-term ecological research. Forest Science Data Bank, Corvallis, OR. http://www.andrewsforest.oregonstate.edu/data/abstract.cfm?dbcode=MS033. Accessed October 05, 2011.

Davison AC, Hinkley DV. 1997. Bootstrap methods and their application. Cambridge Series in Statistical and Probabilistic Mathematics. Cambridge: Cambridge University Press.

Duursma RA, Marshall JD, Robinson AP, Pangle RE. 2007. Description and test of a simple process-based model of forest growth for mixed-species stands. Ecol Model 203:297–311.

Dyrness C. 2001. Soil descriptions and data for soil profiles in the Andrews Experimental Forest, selected reference stands, Research Natural Areas, and National Parks. Long-term ecological research. Forest Science Data Bank, Corvallis, OR. http://www.andrewsforest.oregonstate.edu/data/abstract.cfm?dbcode=SP001. Accessed October 05, 2011.

Dyrness C, Norgren J, Lienkaemper G. 2005. Soil survey (1964, revised in 1994), Andrews Experimental Forest. Long-Term Ecological Research. Forest Science Data Bank, Corvallis, OR. http://www.andrewsforest.oregonstate.edu/data/abstract.cfm?dbcode=SP026. Accessed October 05, 2011.

Elmqvist T, Folke C, Nyström M, Peterson G, Bengtsson J, Walker B, Norberg J. 2003. Response diversity, ecosystem change, and resilience. Front Ecol Envrion 1:488–94.

Franklin JF, Spies TA, van Pelt R, Carey AB, Thornburgh DA, Berg DR, Lindenmayer DB, Harmon ME, Keeton WS, Shaw DC, Bible K, Chen J. 2002. Disturbances and structural development of natural forest ecosystems with silvicultural implications, using Douglas-fir forests as an example. For Ecol Manage 155:399–423.

Govind A, Chen JM, Bernier P, Margolis H, Guindon L, Beaudoin A. 2011. Spatially distributed modeling of the long-term carbon balance of a boreal landscape. Ecol Model 222:2780–95.

Grimm V, Revilla E, Berger U, Jeltsch F, Mooij WM, Railsback SF, Thulke HH, Weiner J, Wiegand T, DeAngelis DL. 2005. Pattern-oriented modeling of agent-based complex systems: lessons from ecology. Science 310:987–91.

Güneralp B, Gertner G. 2007. Feedback loop dominance analysis of two tree mortality models: relationship between structure and behavior. Tree Physiol 27:269–80.

Hardiman BS, Bohrer G, Gough CM, Vogel CS, Curtis PS. 2011. The role of canopy structural complexity in wood net primary production of a maturing northern deciduous forest. Ecology 92:1818–27.

Harmon M, Munger T. 2005. Tree growth and mortality measurements in long-term permanent vegetation plots in the Pacific Northwest (LTER Reference Stands). Long-term ecological research. Forest Science Data Bank, Corvallis, OR. http://www.andrewsforest.oregonstate.edu/data/abstract.cfm?dbcode=TV010. Accessed October 05, 2011.

Hooper DU, Vitousek PM. 1997. The effects of plant composition and diversity on ecosystem processes. Science 277:1302–5.

Huston MA, Marland G. 2003. Carbon management and biodiversity. J Environ Manage 67:77–86.

Jaeger JAG. 2000. Landscape division, splitting index, and effective mesh size: new measures of landscape fragmentation. Landscape Ecol 15:115–30.

Jenkins JC, Chojnacky DC, Heath LS, Birdsey RA. 2004. Comprehensive database of diameter-based biomass regressions for North American tree species. GTR-NE-319, US Department of Agriculture, Newtown Square, PA. 45 pp.

Kane VR, McGaughey RJ, Bakker JD, Gersonde RF, Lutz JA, Franklin JF. 2010. Comparisons between field- and LiDAR-based measures of stand structural complexity. Can J For Res 40:761–73.

Kane VR, Gersonde RF, Lutz JA, McGaughey RJ, Bakker JD, Franklin JF. 2011. Patch dynamics and the development of structural and spatial heterogeneity in Pacific Northwest forests. Can J For Res 41:2276–91.

Kätterer T, Andren O. 2001. The ICBM family of analytically solved models of soil carbon, nitrogen and microbial biomass

dynamics—descriptions and application examples. Ecol Model 136:191–207.

Kaufman L, Rousseeuw PJ. 1990. Finding groups in data: an introduction to cluster analysis. New York: Wiley. 342 pp.

Landsberg JJ, Waring RH. 1997. A generalised model of forest productivity using simplified concepts of radiation-use efficiency, carbon balance and partitioning. For Ecol Manage 95:209–28.

Lefsky MA, Cohen WB, Parker GG, Harding DJ. 2002. Lidar remote sensing for ecosystem studies. Bioscience 52:19–30.

Lefsky MA, Turner DP, Guzy M, Cohen WB. 2005. Combining lidar estimates of aboveground biomass and Landsat estimates of stand age for spatially extensive validation of modeled forest productivity. Remote Sens Environ 95:549–58.

Levin SA. 1998. Ecosystems and the biosphere as complex adaptive systems. Ecosystems 1:431–6.

Lienkaemper G. 2004. Managed stands—harvest year. Original GIS Data Catalog for Andrews Experimental Forest. http://www.andrewsforest.oregonstate.edu/data/spatial/gislist.cfm?-topnav=91. Accessed October 05, 2011.

Lischke H, Löffler TJ. 2006. Intra-specific density dependence is required to maintain species diversity in spatio-temporal forest simulations with reproduction. Ecol Model 198:341–61.

MacDonald GM, Case RA. 2005. Variations in the Pacific Decadal Oscillation over the past millennium. Geophys Res Lett 32:L08703.

McGarigal K, Cushman SA, Neel MC, Ene E. 2002. FRAGSTATS: Spatial Pattern Analysis Program for Categorical Maps. Computer software program produced by the authors at the University of Massachusetts, Amherst. http://www.umass.edu/landeco/research/fragstats/fragstats.html. Accessed October 05, 2011.

McGaughey RJ. 2011. FUSION. Providing fast, efficient, and flexible access to LIDAR, IFSAR and terrain datasets. Pacific Northwest Research Station, US Department of Agriculture. http://www.forsys.cfr.washington.edu/fusion/fusionlatest.html. Accessed October 05, 2011.

McKinley DC, Ryan MG, Birdsey RA, Giardina CP, Harmon ME, Heath LS, Houghton RA, Jackson RB, Morrison JF, Murray BC, Pataki DE, Skog KE. 2011. A synthesis of current knowledge on forests and carbon storage in the United States. Ecol Appl 21:1902–24.

Means JE, Hansen HA, Koerper GJ, Alaback PB, Klopsch MW. 1994. Software for computing plant biomass—BIOPAK Users Guide. PNW-GTR-340, US Department of Agriculture, Portland, OR. 184 pp.

Meinshausen M, Smith SJ, Calvin K, Daniel JS, Kainuma MLT, Lamarque JF, Matsumoto K, Montzka SA, Raper SCB, Riahi K, Thomson A, Velders GJM, van Vuuren DPP. 2011. The RCP greenhouse gas concentrations and their extensions from 1765 to 2300. Clim Change 109:213–41.

Nitschke CR, Innes JL. 2008. A tree and climate assessment tool for modelling ecosystem response to climate change. Ecol Model 210:263–77.

Ohmann JL, Gregory MJ, Henderson EB, Roberts HM. 2011. Mapping gradients of community composition with nearest-neighbour imputation: extending plot data for landscape analysis. J Veg Sci 22:660–76.

Pan Y, Birdsey RA, Fang J, Houghton R, Kauppi PE, Kurz WA, Phillips OL, Shvidenko A, Lewis SL, Canadell JG, Ciais P, Jackson RB, Pacala SW, McGuire AD, Piao S, Rautiainen A, Sitch S, Hayes D. 2011. A large and persistent carbon sink in the world's forests. Science 333:988–93.

Parker GG, Harmon ME, Lefsky MA, Chen J, van Pelt R, Weis SB, Thomas SC, Winner WE, Shaw DC, Franklin JF. 2004. Three-dimensional structure of an oldgrowth Pseudotsuga–Tsuga canopy and its implications for radiation balance, microclimate, and gas exchange. Ecosystems 7:440–53.

R Development Core Team. 2011. R: A language and environment for statistical computing. R Foundation for Statistical Computing, Vienna, Austria. ISBN 3-900051-07-0. http://www.R-project.org/. Accessed October 05, 2011.

Rammig A, Fahse L, Bugmann H, Bebi P. 2006. Forest regeneration after disturbance: a modelling study for the Swiss Alps. For Ecol Manage 222:123–36.

Runyon J, Waring RH, Goward SN, Welles JM. 1994. Environmental limits on net primary production and light-use efficiency across the Oregon transect. Ecol Appl 4:226–37.

Seidl R, Rammer W, Jäger D, Currie WS, Lexer MJ. 2007. Assessing trade-offs between carbon sequestration and timber production within a framework of multi-purpose forestry in Austria. For Ecol Manage 248:64–79.

Seidl R, Rammer W, Bellos P, Hochbichler E, Lexer MJ. 2010. Testing generalized allometries in allocation modeling within an individual-based simulation framework. Trees 24:139–50.

Seidl R, Schelhaas MJ, Lexer MJ. 2011. Unraveling the drivers of intensifying forest disturbance regimes in Europe. Glob Change Biol 17:2842–52.

Seidl R, Rammer W, Scheller RM, Spies TA. 2012. An individual-based process model to simulate landscape-scale forest ecosystem dynamics. Ecol Model 231:87–100.

Smithwick EAH, Harmon ME, Remillard SM, Acker SA, Franklin JF. 2002. Potential upper bounds of carbon stores in forests of the Pacific Northwest. Ecol Appl 12:1303–17.

Smithwick EAH, Harmon ME, Domingo JB. 2003. Modeling multiscale effects of light limitations and edge-induced mortality on carbon stores in forest landscapes. Landscape Ecol 18:701–21.

Spies TA, Franklin JF. 1988. Old-growth and forest dynamics in the Douglas-fir region of western Oregon and Washington. Nat Areas J 8:190–201.

Spies TA, Franklin JF, Thomas TB. 1988. Coarse woody debris in Douglas-fire forests of western Oregon and Washington. Ecology 69:1689–702.

Spies TA, McComb BC, Kennedy RSH, McGrath MT, Olsen K, Pabst RJ. 2007. Potential effects of forest policies on terrestrial biodiversity in a multi-ownership province. Ecol Appl 17:48–65.

Stegen JC, Swenson NG, Enquist BJ, White EP, Phillips OL, Jorgensen PM, Weiser MD, Mendoza AM, Vargas PN. 2011. Variation in above-ground forest biomass across broad climatic gradients. Glob Ecol Biogeogr 20:744–54.

Tague C, Heyn K, Christensen L. 2009. Topographic controls on spatial patterns of conifer transpiration and net primary productivity under climate warming in mountain ecosystems. Ecohydrology 2:541–54.

Teensma PDA. 1987. Fire history and fire regimes of the central western Cascades of Oregon. Dissertation, University of Oregon. 188 pp.

Tepley AJ. 2010. Age structure, developmental pathways, and fire regime characterization of Douglas-fir/Western Hemlock Forests in the Central Western Cascades of Oregon. Dissertation, Oregon State University. 278 pp.

Turner DP, Dodson R, Marks D. 1996. Comparison of alternative spatial resolutions in the application of a spatially distributed

biogeochemical model over complex terrain. Ecol Model 90:53–67.

Turner DP, Guzy M, Lefsky MA, van Tuly S, Sun O, Daly C, Law BE. 2003. Effects of land use and fine-scale environmental heterogeneity on net ecosystem production over a temperate coniferous forest landscape. Tellus 55B:657–68.

Weisberg PJ, Swanson FJ. 2003. Regional synchroneity in fire regimes of western Oregon and Washington, USA. For Ecol Manage 172:17–28.

Wu J, David JL. 2002. A spatially explicit hierarchical approach to modeling complex ecological systems: theory and applications. Ecol Model 153:7–26.

Yachi S, Loreau M. 2007. Does complementary resource use enhance ecosystem functioning? A model of light competition in plant communities. Ecol Lett 10:54–62.